

THEORETICAL CONSIDERATIONS ON A 2D COMPLIANT TENSEGRITY JOINT IN CONTEXT OF A BIOMEDICAL APPLICATION

Leon Schaeffer¹, David Herrmann¹, Valter Böhm¹

¹OTH Regensburg, Faculty of Mechanical Engineering

ABSTRACT

In this paper, a two-dimensional compliant tensegrity joint was investigated for potential biomedical applications such as orthotics or exoskeletons. The structure consists of two compressed members connected by five compliant tensioned members. The concept is based on the tensegrity principle, which allows the realization of dynamic orthoses without conventional hinge joints. Another advantage is the adaptability to the individual needs of the patient through a suitable design of the structure and the careful selection of the characteristics of the elements. Using geometric nonlinear analysis, the mechanical behavior of the structure was investigated, focusing on mechanical compliance. The main objective was to determine the influence of the initial length and stiffness of the tensioned members and the influence of the magnitude of external forces on the overall stiffness of the movable member of the structure. The results highlight the significant impact of member parameters on the structure's stiffness and movability under varying load magnitudes. The research laid the foundation for future development of dynamic orthoses based on this structure.

Index Terms - Tensegrity Joint, Flexibility Ellipsis, Mechanical Compliance

1. INTRODUCTION

The idea of using mechanically prestressed compliant structures in biomedical applications appears to be innovative in several respects [1], [2]. By changing the amount of prestress, the desired stiffness of these structures could be changed significantly. This can be realized even without changing the shape of the structures. Compliant tensegrity structures constitute a special class of mechanically prestressed structures. They are formed by a set of disconnected compressed members connected with a continuous net of compliant tensioned members with high elasticity by pin joints. Those structures consist in most cases only of one-dimensional members. According to the tensegrity principle, the compressed members are connected to each other only by tensioned members. The resulting shape of these structures is defined by the balance between the tensile and compressive forces of the members. Due to the prestress state, tensegrity structures enable freestanding self-stable equilibrium configurations.

The human hand and wrist are anatomically one of the most complex regions of the human body. This characteristic is following due to the complex structure of bones, joints, tendons, and ligaments which are interconnected in a very confined space. Stress related hand injuries that occur must therefore be treated quickly and adequately with appropriate therapies to restore hand function.

Orthoses present challenges in terms of accessibility for medical interventions due to their enclosed design. Additionally, some current orthoses tend to be heavy and bulky due to the size and weight of their components. Furthermore, existing orthoses have limited adjustability, often



allowing adjustments in only a single degree of freedom or to a small extent. Another limitation of current orthoses is their restricted range of motion, which often does not cover the maximum anatomically permissible range. In certain situations, it may be beneficial to have an orthosis that allows for an enhanced range of motion. The consideration of compliant tensegrity structures in the context of biomedical applications, especially as a basis for dynamic orthoses, is therefore promising. The adaptation of these structures to specific tasks can be realized by proper selection of the individual stiffness and length of the structure's members.

In the present paper, a two-dimensional compliant tensegrity joint is investigated in context for possible further biomedical applications such as orthoses or exoskeletons. The structure consists of only two rigid compressed members, which are connected by five compliant tensioned members. Those structures are usually realized by springs with constant stiffness [3]–[5]. Different approaches to realize the tensioned members by elastomers are given in [6], [7]. The considered structure enables a great shape change capability. To analyze the mechanical behavior of the structure, the use of geometric nonlinear analysis is required. Due to this nonlinearity, the structural behavior is hardly predictable without detailed theoretical investigations.

In this work, the overall static mechanical behavior with focus on the mechanical compliance of the considered structure will be analyzed with the help of geometric nonlinear static finite-element simulations in dependence of structural parameters. These investigations build the basis for the future development of dynamic orthoses based on this structure.

At the beginning of this paper, the main characteristics of prestressed compliant structures are discussed in Section 2. In Section 3, the two-dimensional prestressed compliant joint structure used for the characterization analysis is described. The main part of the work in Section 4 deals with the overall stiffness behavior when varying different properties of the structure members or the magnitude of the externally applied forces. The results of this analysis are discussed in Section 5. At the end, a conclusion and an outlook for further investigations is given.

2. PRESTRESSED COMPLIANT STRUCTURES

Compliant tensegrity structures represent a unique subset of mechanically prestressed systems. Traditional tensegrity structures, exclusively composed of bars experiencing uniaxial compression (compressed members) and wires subjected to uniaxial tension (tensioned members), display a unique combination of these structural members. Their overall shape and mechanical stiffness are primarily determined by the prestress state, influenced by the topology (connectivity) and properties (such as stiffness and initial length) of each constituent member. As an example, in Figure 1 a simple 3D conventional tensegrity structure is shown. This approach enables precise control over the overall structural behavior and allows tailored designs with optimized mechanical performance.

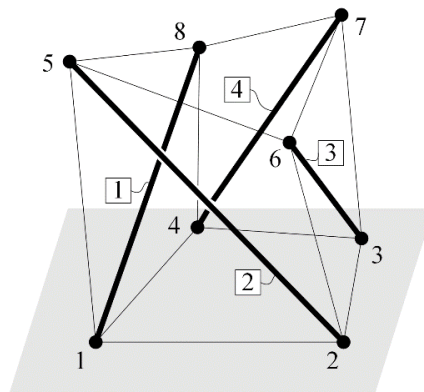


Figure 1: A simple 3D tensegrity structure consisting of four compressed members (thick lines) and twelve tensioned members (thin lines).

Tensegrity structures, with their exceptional properties of deployability, lightweight design, high load-to-weight ratio, and impressive shock-absorbing capabilities, have found increasing applications in robotics and civil engineering. They offer structural flexibility, adaptability to dynamic environments, and inherent robustness to external perturbations. Furthermore, their unique combination of strength and flexibility makes them suitable for diverse fields such as aerospace engineering, biomechanics, and structural systems [6], [8]–[12]. Using compliant tensegrity structures in biomedical applications, particularly as a basis for dynamic orthoses, holds significant promise based on the following key aspects:

- These structures offer the advantage of implementing mechanisms without conventional joints, allowing for multiple joint axes where the corresponding pivot points and rotary axes can be located external to the structure. This design approach allows for the alignment of joint pivot points and rotary axes with anatomically predefined positions, offering improved functionality and natural movement.
- The minimal number of members in tensegrity structures allows for unobstructed joint areas, providing ample space for the intended purpose and therefore offering enhanced comfort and mobility for the user.
- The overall stiffness of tensegrity structures can be precisely controlled by proper selection of mechanical parameters such as the initial length and stiffness of individual members and applying appropriate prestress.
- The reversible adjustability of the prestress level allows for reversible adjustments in stiffness, even without altering the fundamental shape, allowing for flexibility in adapting to changing conditions or desired stiffness preferences.

3. TWO-DIMENSIONAL COMPLIANT TENSEGRITY JOINT

In the following, a two-dimensional compliant tensegrity joint will be introduced and considered for feasibility and technical implementation. The joint is based on the well-known simple two-dimensional tensegrity structure (Figure 2a). It consists of two rigid compressed members (CM_I , CM_{II}) and four compliant tensioned members ($4 \times TM_I$). Each end point of one compressed member is connected with both end points of the other compressed member through the tensioned members by pin-joints. The compressed members are interconnected indirectly only through the tensioned members. In this manner, relative movement between the compressed members is possible in all three directions (translation in x- and y-direction and rotation about the z-axis) due to the elasticity of the tensioned members. The structure is freestanding. Static equilibrium is achieved without applying any geometrical boundary conditions.



Figure 2: 2D tensegrity structure (compressed members: thick black lines, compliant tensioned members: thin blue lines); a) connectivity of the members; b) static equilibrium configuration in case of applying tensioned members TM_I with identical parameters.

The member's parameters (lengths and stiffnesses) define the shape of the structure in the equilibrium configuration. For identical parameters of the tensioned members, the resulting shape corresponds to a double symmetrical cross (Figure 2b). By suitable selection of the properties of the tensioned members (length, stiffness) as well as length of the compressed members, the relative position between the two compressed members can be defined. Because the length of the tensioned members in the equilibrium state of the structure is larger than in their initial state without any loads, the structure is in a prestressed state. The overall prestress of the structure is defined by the member's parameters (initial length and stiffness of the tensioned members). By applying additional tensioned members, both the stiffness of the overall structure and the relative position between both compression members can be easily modified. In Figure 3 thereby modified prestressed compliant joint structure with an additional tensioned member TM_{II} is shown which is connected to the end point 3 of the compressed member CM_{II} . The other end point 5 is fixed in the plane.

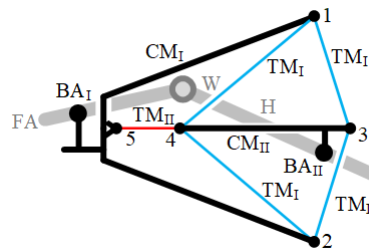


Figure 3: 2D tensegrity structure with a V-shaped compressed member in combination with the wrist region; FA: forearm, W: wrist joint, H: hand, BA_I : connection point between CM_I and FA, BA_{II} : connection point between CM_{II} and H.

The fixed points 1, 2, and 5 enable the use of a fixed V-shaped rigid compressed member with three connection points instead of the straight compressed member CM_I . This specific design allows for a wide range of movement for CM_{II} without colliding with CM_I . As a result, the structure consists of two rigid members capable of relative movement without conventional joints. The applied forces determine the magnitude of the relative motion, which is associated with the stiffness of the structure. As an example, for a hand orthosis, it is preferable to connect the V-shaped compressed member CM_I to the forearm (FA) and the compressed member CM_{II} to the hand (H) at connection points BA_I and BA_{II} , respectively, placing the wrist joint (W) within the orthosis structure. This configuration allows for flexion and extension of the hand, while the individual stiffness of the prestressed compliant joint structure ensures adaptability. However, the range of motion is limited by the potential collision between the distal and palmar sides of the hand and the end points 1 and 2 of the V-shaped compressed member CM_I .

4. CHARACTERISTICS ANALYSIS

In the following, the overall stiffness of the prestressed 2D compliant joint is investigated by performing a characteristics analysis. The characteristics analysis is based on the form-finding algorithm described in [9]. This algorithm is a modified version of the method presented by [13], based on the geometrically non-linear static FEM, and is implemented in Matlab®. In the analysis, the V-shaped rigid compressed member is fixed. Therefore, the nodes 3,4,5 are fixed, and this member is neglected. In the first step of the characteristic analysis, the static equilibrium state of the structure is determined without any external load by neglecting weight forces. This state can be characterized by the center point of the movable compressed member and their orientation in the plane. In a subsequent step, external forces of equal magnitude and identical orientation are applied to nodes 1 and 2. By varying the orientation of the forces in the range of $0 \dots 360^\circ$ plotting the positions of the center point of the movable compressed member for all force orientations and by connecting these points, a closed curve can be drawn. For small

forces, the shape of this closed curve corresponds to an ellipsis. This ellipsis is called as flexibility ellipsis. This ellipsis characterizes the overall stiffness of the structure, showing the directions of smaller and larger stiffness. By varying of the parameters of the members and load magnitude, the shape of this closed curve and the size of the enclosed area can be influenced in a wide range. Thus, the overall stiffness of the structure can be defined with an appropriate choice of mechanical parameters of the tensioned members (initial length in the unstressed state and stiffness).

In Figure 4, the investigated structure is shown in its stable equilibrium position after the form-finding process. The figure shows the behavior of the overall stiffness of the structure in a fully symmetrical case (each tensioned member has the same initial length ($L = 10$ mm) and stiffness ($k = 0.4$ N/mm)). The length of the movable compressed member is $a = 100$ mm. The end points of this member correspond to nodes 1 and 2. The coordinates of the fixed nodes 3, 4, 5 are: $x_3 = x_4 = 0$, $y_3 = -y_4 = a/2$, $x_5 = -a$, $y_5 = 0$.

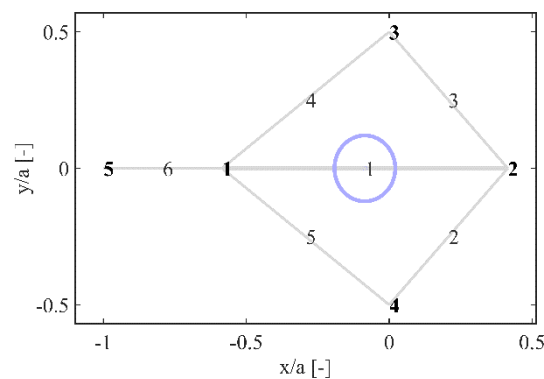


Figure 4: Overall displacement behavior for the prestressed compliant joint structure in a fully symmetrical case (light gray: stable equilibrium position of structure, light blue: trajectory curve of middle point of movable compressed member, member parameter: $k = 0.4$ N/mm, $L = 10$ mm, $F = 10$ N)

As the results show, the directional stiffness of the structure is symmetric, due to the symmetric arrangement and member properties. In the following, selected results are presented to illustrate the variability in stiffness when the structure's symmetry is disrupted.

4.1 Variation of individual member stiffness

In the following, the symmetry is disturbed by altering the initial stiffness of one member at a time. Seven stiffness levels are considered (0.01, 0.1, 0.4, 0.8, 1.6, 2, and 4 N/mm), while the stiffness of the other four tensioned members remains constant at $k = 0.4$ N/mm. All tensioned members have a length of $L = 10$ mm, and an external force of $F = 10$ N is applied on nodes 1 and 2.

Figure 5a demonstrates the structural behavior by stiffness-variation of the second tensioned member. Smaller stiffness values ($k = 0.01$ and $k = 0.1$ N/mm – dark blue markers) for this member allow for greater displacement of the movable compressed member from its initial position, resulting in a larger enclosed area of the trajectory curve compared to cases where the second tensioned member has higher stiffness values ($k = 0.8$, $k = 1.6$, $k = 2$, $k = 4$ N/mm) than the others. Higher stiffness values ($k = 0.8$, $k = 1.6$ N/mm) yield an enclosed trajectory curve that approximates a circle, while stiffness values of $k = 2$ and $k = 4$ N/mm result in a trajectory curve with a triangular shape and circular edges. The trajectory of the centroids of each surface traces a crescent-shaped curve, with the closed curve side oriented towards members 2 and 3, and the open side directed towards members 4, 5, and 6. At the midpoint, characterized by $k = 0.4$ N/mm, the trajectory of the centroids of each surface can be virtually divided, with the upper portion displaying a larger aperture compared to the lower portion. In the lower half, the center points of each iteration lie closer together than in the upper half. The structural behavior

exhibits symmetry with respect to the x-axis by stiffness variation of the second or third tensioned members (see Figure 5a and Figure 5b). This symmetrical behavior is evident also for all tensioned member's variations that have a corresponding symmetrical counterpart, as depicted in Figure 5d and Figure 5e.

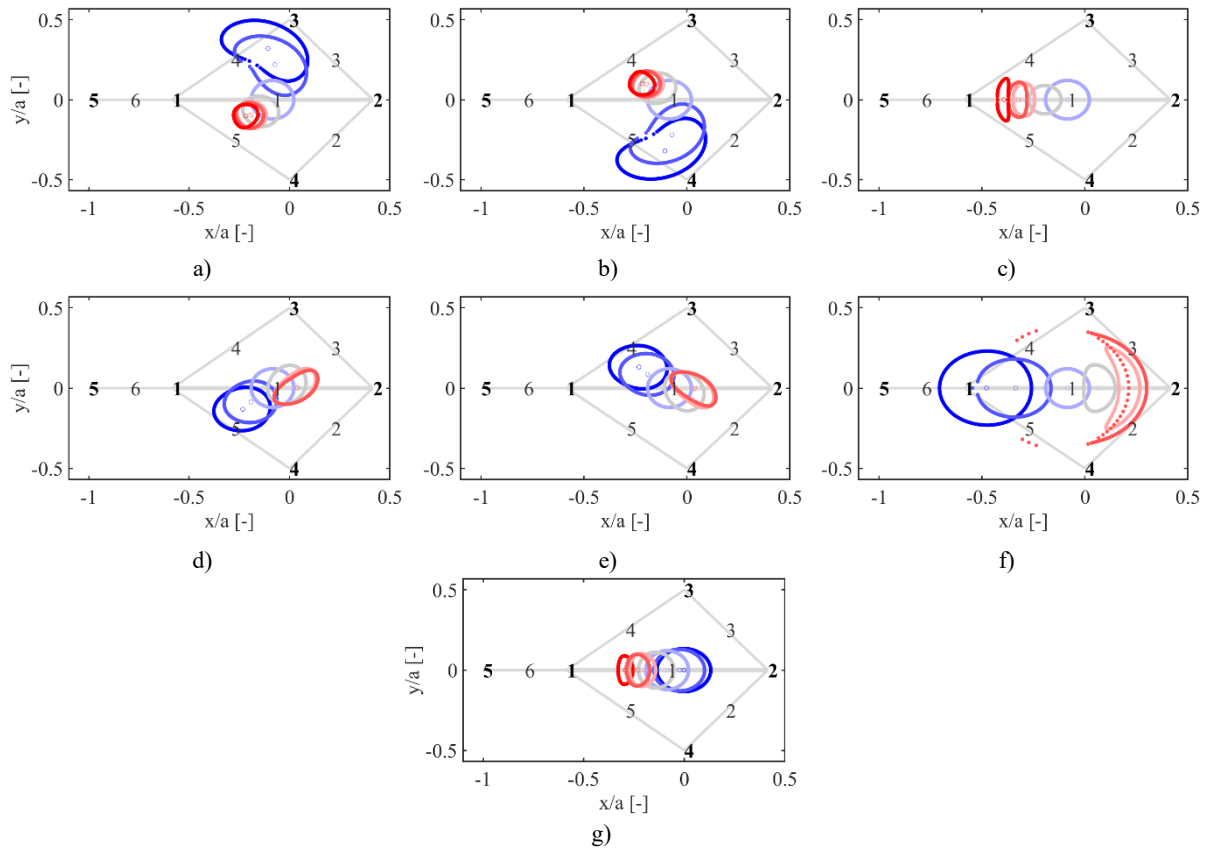


Figure 5: Displacement of the middle point of the movable compressed member by variation of the stiffness of selected tensioned members: a) member 2, b) member 3, c) members 2 and 3, d) member 4, e) member 5, f) member 4 and 5 and g) member 6 (dark blue – light blue – dark gray – gray – light gray – light red – dark red: stiffness values from 0.01 N/mm to 4 N/mm).

The behavior of the overall stiffness of the structure when two pairs of symmetrical arranged tensioned members are varied to the rest of the tensioned members is shown in Figure 5c. In the depicted example, the stiffnesses of tensioned members 2 and 3 are simultaneously varied. As the stiffness of the tensioned members increases, the enclosed area transforms from a nearly symmetrical circle at $k = 0.4$ N/mm to an ellipse. The major axis of the ellipse is oriented vertically, while the length of the minor axis, oriented horizontally, decreases with stiffer tensioned members. At a stiffness of $k = 4$ N/mm, the ellipse takes on a convex shape with its straight side facing members 2 and 3, indicating lower vertical stiffness compared to horizontal stiffness for this parameter set. Trajectory curves for stiffnesses of $k = 0.01$ N/mm and $k = 0.1$ N/mm are excluded since no singular results can be obtained. This effect is also observed in the trajectory curve for a stiffness of 4 N/mm.

In Figure 5d and Figure 5e, the structural behavior is shown when changing the stiffness of member 4 or member 5. For a small stiffness value $k = 0.01$ N/mm, the enclosed area is equivalent to an ellipse with its major axis oriented horizontally, nearly parallel to the movable compressed member. The center point of the enclosed area sits below the movable compressed member in its initial equilibrium position, with a slight angle to its orientation and the left endpoint tilted away from the movable compressed member more than the right endpoint. The minor axis is only slightly shorter than the major axis. With increasing stiffness, the ellipse becomes less tilted. Initially, higher stiffness values yield increased tilt angles, but with further

increases in stiffness, the angle decreases again. The maximum tilt is reached at $k = 0.8 \text{ N/mm}$. The center point of these ellipses ($k = 0.8, k = 1.6, k = 2,$ and $k = 4 \text{ N/mm}$) is at nearly the same height as for $k = 0.4 \text{ N/mm}$. The side of the ellipse closer to the varied tensioned members exhibits a larger curvature, while the other side shows less curvature. With higher stiffness values, the overall stiffness of the structure decreases, and a directional dependence can be observed.

Figure 5f illustrates the overall stiffness behavior when the stiffness of members 4 and 5 is varied simultaneously. Similar to the case of members 2 and 3 in Figure 5c, trajectory curves for stiffness of $k = 4 \text{ N/mm}$ are excluded since no singular results can be obtained. The loss of data points for certain angles of the external force is already evident at a stiffness of $k = 1.6 \text{ N/mm}$. In general, the overall stiffness of the structure increases symmetrically for larger stiffnesses of individual members. For higher stiffnesses of members 4 and 5, the trajectory curve transforms into a vertical oriented ellipse at $k = 0.8 \text{ N/mm}$. At a stiffness of $k = 1.6 \text{ N/mm}$, the ellipse further transforms into a crescent-shaped ellipse.

Figure 5g shows the overall structural behavior when the stiffness of member 6 is changed. For smaller stiffness values ($k = 0.01 \text{ N/mm}$ and $k = 0.1 \text{ N/mm}$) with respect to the default comparison level of $k = 0.4 \text{ N/mm}$, the enclosed area corresponds to slightly larger ellipses than the one at $k = 0.4 \text{ N/mm}$. The overall stiffness is symmetrical in this case, and an even displacement of the movable compressed member can be observed. With increasing stiffness of member 6, the middle point and the enclosed area shift towards the left side, closer to the location of member 6. The enclosed area changes from a semicircular form to an ellipse, with the side closer to member 6 exhibiting a straighter line compared to the other side, which has more curvature. Additionally, the major axis of the ellipse is oriented in the vertical direction. In this case, the overall stiffness of the prestressed compliant structure is stiffer in the horizontal direction than in the vertical direction.

The summary of each individual trajectory curve is shown in Figure 6. As seen from the figures Figure 5a to Figure 5g, the directional stiffness of the structure can be defined in a wide range with proper selection of each member's individual stiffness.

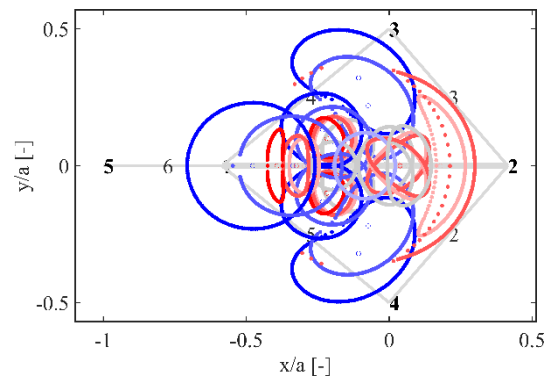


Figure 6: Summary of all individual trajectory curves for the displacement of the middle point of the movable compressed member by variation of the stiffness (dark blue – light blue – dark gray – gray – light gray – light red – dark red: stiffness values from 0.01 N/mm to 4 N/mm).

4.2 Variation of individual members length

In the following, the symmetry is disturbed by altering the initial length of one member at a time. Seven levels of initial member's length are considered (1, 5, 10, 20, 35 and 50 mm), while the length of the other four tensioned members remains constant at $L = 10 \text{ mm}$. All tensioned members have a stiffness of $k = 0.4 \text{ N/mm}$, and an external force of $F = 10 \text{ N}$ is applied on nodes 1 and 2.

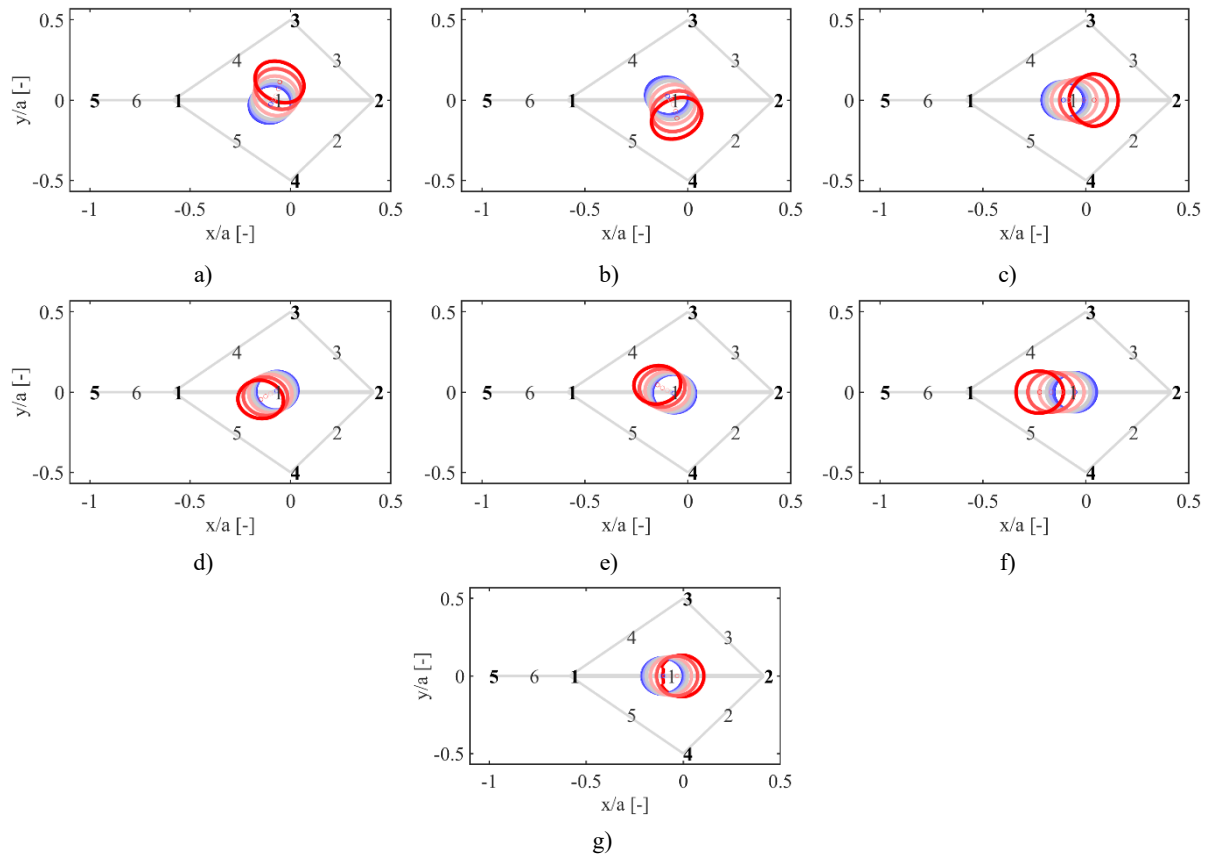


Figure 7: Displacement of the middle point of the movable compressed member by variation of the initial length of selected tensioned members: a) member 2, b) member 3, c) members 2 and 3, d) member 4, e) member 5, f) member 4 and 5 and g) member 6 (dark blue – light blue – dark gray – gray – light gray – light red – dark red: lengths values from 1 mm to 50 mm).

Figure 7a demonstrates the overall stiffness behavior of the structure when varying the initial length of the tensioned member 2. For short initial member's length (1, 5 and 10 mm – dark blue to dark gray markers) only a moderate displacement of the movable compressed member from its initial position is possible. For short lengths, the form of the enclosed area yields an enclosed trajectory curve that approximates a circle with a smaller enclosed area compared to cases with longer initial lengths such as $L = 20$, $L = 35$ and $L = 50$ mm. With increasing length, the form of the enclosed area transforms into a more elliptical form. The major axis of the ellipses is thereby tilted upward. The total enclosed area is larger than for smaller lengths, indicating a greater overall movability of the prestressed compliant structure. The trajectory of the centroids of each enclosed area traces an upward facing curve similar to an exponential function, with the inner curve side oriented towards members 4, 5 and 6, and the outside face directed towards members 2 and 3. At the midpoint, characterized by $L = 10$ mm, the trajectory of the centroids of each surface can be virtually divided, with the upper portion displaying a larger aperture compared to the lower portion. In the lower half, the center points of each iteration lie closer together than in the upper half. The structural behavior exhibits symmetry with respect to the x-axis by length variation of the tensioned members 2 and 3 (compare Figure 7a and Figure 7b). This symmetrical behavior is evident also for all tensioned member's variations that have a corresponding symmetrical counterpart, as depicted also in Figure 7d and Figure 7e.

Figure 7c illustrates the overall stiffness of the movable compressed member of the structure when the initial length of the members 2 and 3 is varied simultaneously. The trajectory curves and their respective center points all align collinearly with the x-axis. The leftmost trajectory curve which forms an ellipse with its major axis identical to the x-axis corresponds to a

member's initial length of 1 mm, the rightmost flexibility ellipse formed by the trajectory curve corresponds to a member's initial length of $L = 50$ mm. The form of this ellipse is close to a circle. In between the initial length of $L = 1$ mm and $L = 50$ mm, the areas of the enclosed trajectory curves increase slightly. This characteristic indicates a greater movability for longer initial lengths than for shorter lengths for members 2 and 3. For longer initial lengths, the overall position of the movable compressed member is shifted to the right.

In Figure 7c and Figure 7d, the corresponding mechanical behavior regarding the overall stiffness of the structure is shown for different initial lengths of the tensioned members 4 and 5. The structural behavior exhibits symmetry with respect to the x-axis by length variation of the tensioned members 4 and 5. Increasing the initial untensioned length of the members from $L = 1$ mm to $L = 50$ mm results in symmetrical increases in the enclosed area formed by the trajectory curves. This indicates a decrease in overall structure stiffness when the initial member's length is increased. The centroids of each enclosed area are aligned along a straight line with a positive slope. The lowest center point on the line thereby corresponds to an initial member's length of $L = 50$ mm.

In Figure 7f, the overall stiffness behavior of the movable compressed member is shown when the initial length of the members 4 and 5 is varied simultaneously. Starting at 1 mm, being the furthest to the right side, the form of the enclosed area, indicating the overall stiffness of the structure, is elliptical. The major axis of the ellipses is parallel to the x-axis. Increasing the initial untensioned length of the members from $L = 1$ mm to $L = 50$ mm yields in a symmetrical increase of the enclosed area of the trajectory cure. The flexibility ellipse furthest to the left is linked to an initial member's length of $L = 50$ mm. The form of the enclosed area for $L = 50$ mm is also an ellipsis, with its major axis being parallel to the x-axis. The center points of the trajectory curves for each variation align along the x-axis. For longer initial lengths, the overall position of the movable compressed member is shifted to the left.

In Figure 7g, the overall stiffness of the structure is presented when varying the initial lengths of the member 6 of the structure. The trajectory curves and their respective center points all align collinearly with the x-axis. The leftmost trajectory curve, forming an ellipse, corresponds to an initial member length of $L = 1$ mm. The rightmost trajectory curve corresponds to a member's initial length of $L = 50$ mm. The enclosed area slightly increases, indicating greater movability of the movable compressed member for longer initial lengths of member 6. The overall behavior is like the behavior of the structure when varying the length of the members 2 and 3 but with smaller increase of the enclosed area while varying the member 6 of the structure. The summary of each individual trajectory curve is shown in Figure 8. As seen from the figures Figure 7a to Figure 7g, the directional stiffness of the structure can be defined in a wide range with proper selection of each member's individual length.

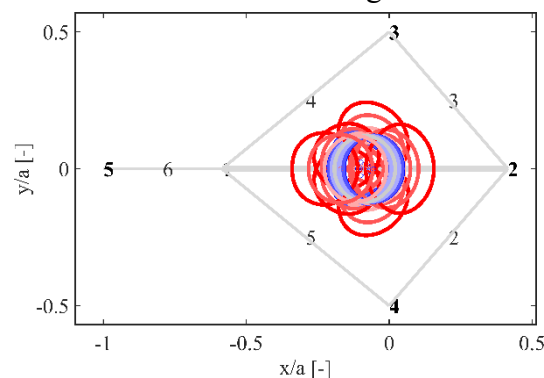


Figure 8: Summary of all individual trajectory curves for the displacement of the middle point of the movable compressed member by variation of the initial member's length (dark blue – light blue – dark gray – gray – light gray – light red – dark red: stiffness values from 0.01 N/mm to 4 N/mm).

4.3 External Force

In this section, the influence of the external force magnitude on the overall stiffness of the structure is investigated. For the fully symmetrical case for $k = 0.4 \text{ N/mm}$ for all tensioned members with an initial member's length of $L = 10 \text{ mm}$, the magnitude of the external forces applied to the movable compressed member at the nodes 1 and 2 is varied in seven levels (1, 5, 10, 15, 20, 35 and 50 N). The corresponding plot with the flexibility ellipse for these seven different levels of external forces can be seen in Figure 9.

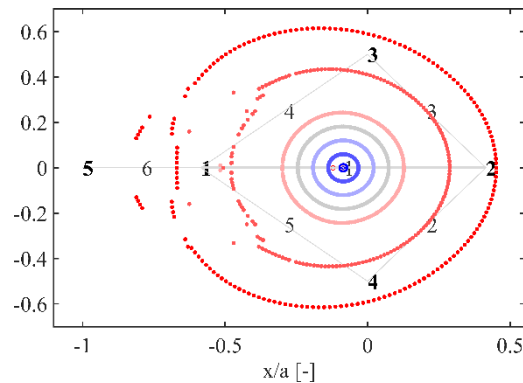


Figure 9: Overall displacement behavior for the prestressed compliant joint structure in a fully symmetrical case ($k = 0.4 \text{ N/mm}$, $L = 10 \text{ mm}$, $F = 10 \text{ N}$) for different magnitudes of external force applied on nodes 1 and 2 of the movable compressed member (dark blue – light blue – dark gray – gray – light gray – light red – dark red: force values from 1 N to 50 N).

In the following, the symmetry of the structure is disturbed by altering the stiffness of three individual sets of members (members 2 and 3, members 4 and 5 and member 6) at a time while simultaneously varying the magnitude of the external force. The used stiffness levels are $k = 0.1 \text{ N/mm}$, $k = 1.6 \text{ N/mm}$, and $k = 4 \text{ N/mm}$. For each stiffness variation, the magnitude of the external force is varied according to the prescribed seven levels. The stiffness of the members which are not varied is set to $k = 0.4 \text{ N/mm}$ and the initial member's length is set to $L = 10 \text{ mm}$.

In Figure 10a to Figure 10c, the influence of different external forces levels for different stiffness values when varied simultaneously at the members 2 and 3 is shown. The form of the enclosed area for low stiffness of $k = 0.1 \text{ N/mm}$ is elliptical for high force levels, while being crescent shaped for low force levels (1 N and 5 N). The open side of the crescent shaped enclosed areas is for all three cases, orientated to the members 2 and 3. With increasing stiffness of the members 2 and 3, the form is shifted to more a vertical orientated elliptical form for low force levels at $k = 1.6 \text{ N/mm}$ while being more crescent shaped for high forces (35 N and 50 N). The centroids of each set are shifted to the left side with increasing stiffness. For stiffnesses of $k = 4 \text{ N/mm}$, only at forces of $F = 1 \text{ N}$ the vertical elliptical form remains. At higher force levels, the crescent shaped is noticeable. In all three variants the movability of the movable compressed member is heavily increased, indicating a lower overall stiffness of the structure. For $k = 1.6 \text{ N/mm}$ and $k = 4 \text{ N/mm}$ all trajectory curves except for $F = 50 \text{ N}$ are fully “closed” and for each angle of applied external force a data point can be traced.

In Figure 10d to Figure 10e the influence of different external forces levels for different stiffness values (0.1 N/mm, 1.6 N/mm, 4 N/mm) when varied simultaneously at the members 4 and 5 is shown. For a low stiffness and high external forces, the shape of the enclosed area resembles ellipses which are elongated and where the first half of the ellipses being closer to members 4 and 5 has a narrower vertical dimension than the second half which is further away from members 4 and 5. For lower externally applied forces, the form of the trajectory curves is shifted more to normally formed ellipses. At higher stiffness levels, the form is shifted to a crescent shaped form with its open side facing the element 4, 5 and 6. With increasing force levels, the

number of fully closed trajectory curves (1.6 N/mm: 3, 4 N/mm: 1) decreases. Overall, the movability increases with increasing force. The centroids of each set are shifted to the right side with increasing stiffness.

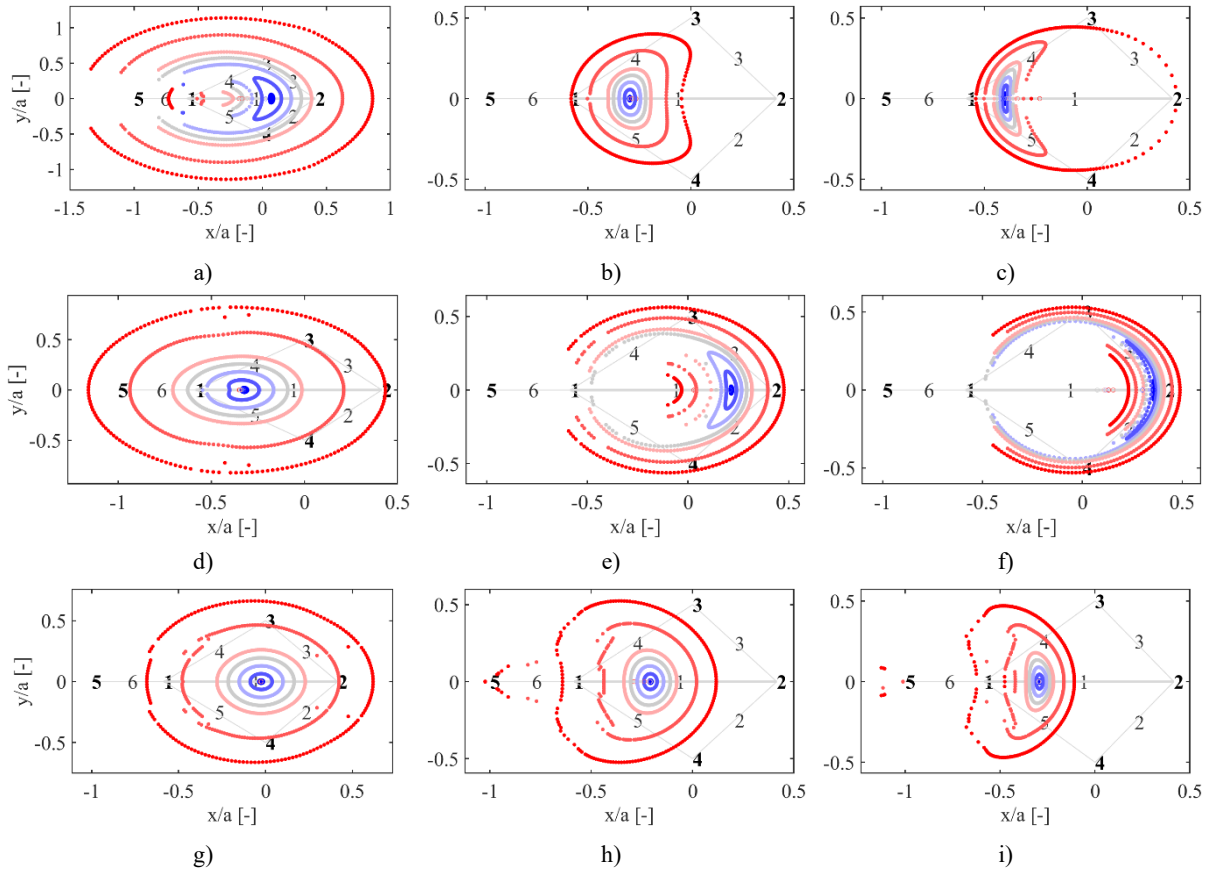


Figure 10: Displacement of the middle point of the movable compressed member by variation of the external force while varying the stiffness of selected tensioned members in 3 levels: a) members 2 and 3 (0.1 N/mm), b) members 2 and 3 (1.6 N/mm), c) members 2 and 3 (4 N/mm), d) members 4 and 5 (0.1 N/mm), e) members 4 and 5 (1.6 N/mm), f) members 4 and 5 (4 N/mm), g) member 6 (0.1 N/mm), h) member 6 (1.6 N/mm) and i) member 6 (4 N/mm) (dark blue – light blue – dark gray – gray – light gray – light red – dark red: force values from 1 N to 50 N).

In Figure 10g to Figure 10i, the influence of different external forces is investigated when varying the stiffness of member 6. For the five smaller forces levels (1, 5, 10, 15, 20) the trajectory curves are fully closed, and the form of the enclosed area is shifting from a horizontally oriented ellipse ($k = 0.1$ N/mm) to more vertical oriented forms for 1.6 N/mm and 4 N/mm. The overall stiffness characteristics of the structure are for all three cases symmetrical. For high force levels $F = 35$ N and $F = 50$ N the overall stiffness changes in all three cases abruptly to a much smaller level, indicating more movability of the movable compressed member. The form of the enclosed area can be described best as bell shaped (“jellyfish-like”) orientated 90° clockwise. The right side of the enclosed area is thereby fully closed while on the left side of the trajectory curve the distances between the data points are larger. The centroids of each set are shifted to the left side with increasing stiffness of tensioned member 6.

In the following, the symmetry of the structure is disturbed by altering the initial member's length of three individual sets of members (members 2 and 3, members 4 and 5 and member 6) at a time while simultaneously varying the magnitude of the external force. The used initial length levels are $L = 1$ mm, $L = 20$ mm, and $L = 45$ mm. For each stiffness variation, the magnitude of the external force is varied according to the prescribed seven levels. The length of the members which are not varied is set to $L = 10$ mm and the stiffness of these members is set to $k = 0.4$ N/mm.

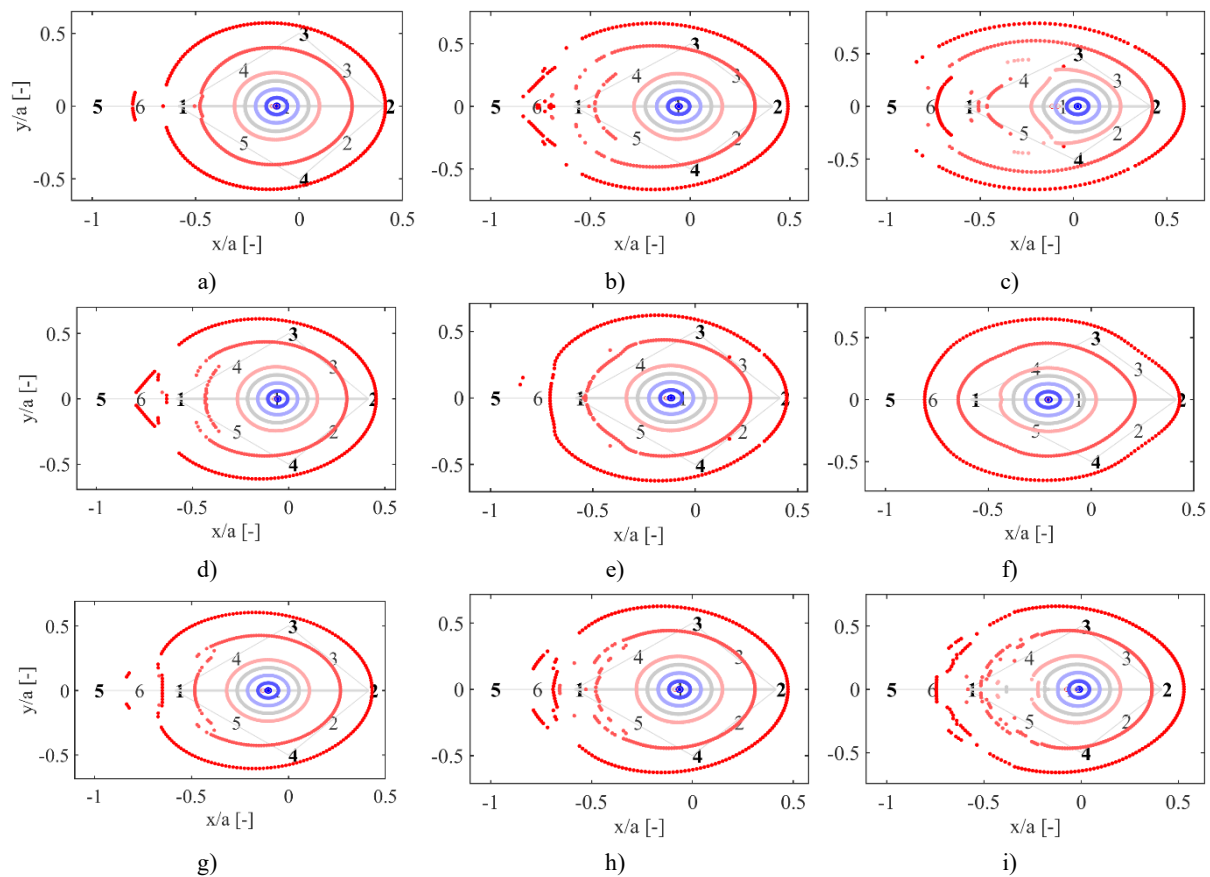


Figure 11: Displacement of the middle point of the movable compressed member by variation of the external force while varying the stiffness of selected tensioned members in 3 levels: a) members 2 and 3 (1 mm), b) members 2 and 3 (20 mm), c) members 2 and 3 (45 mm), d) members 4 and 5 (1 mm), e) members 4 and 5 (20 mm), f) members 4 and 5 (45 mm), g) member 6 (1 mm), h) member 6 (20 mm) and i) member 6 (45 mm) (dark blue – light blue – dark gray – gray – light gray – light red – dark red: force values from 1 N to 50 N).

Figure 11a to Figure 11c shows the influence of different external force levels for different initial member's length values when varied simultaneously on members 2 and 3. The shape of the enclosed area for low initial member's length $L = 1$ mm is elliptical for all force levels. The change of the overall stiffness of the structure is symmetrical for the lower five force levels. For high forces (35 N and 50 N) the overall movability of the structure is heavily increased. On the left side, indicating a force direction of 180° , of both of these ellipses a small part of the ellipses on both side of the x-axis is shifted symmetrical to the inside ($F = 35$ N) and the outside ($F = 50$ N) – indicating the presence of the possibility of multiple equilibrium states. These characteristics must be analyzed in further detailed theoretical investigations. The behavior of the form of the enclosed area is identical for an initial length of $L = 20$ mm. The area on the left side for high forces where the points are shifted away from the main elliptical form is increased, and the points are placed corresponding to a more complex pattern. For the high initial length $L = 45$ mm, this effect already starts at an external force of $F = 20$ N but with only a small portion of the curve being shifted away.

Figure 11d to Figure 11e show the influence of different external force levels for different initial length values (1 mm, 20 mm and 45 mm) when varied simultaneously at members 4 and 5. The shape of the enclosed area for low initial member's length $L = 1$ mm is elliptical for all force magnitudes. For high forces (35 N and 50 N) the overall movability of the structure is heavily increased. For high force magnitudes at longer initial members length, the trajectory curves are almost fully closed with only a few data points shifted away. For long initial length and high external force magnitude of $F = 35$ N, the form of the enclosed area is elongated where the first

half of the ellipses being closer to member 6 has a narrower vertical dimension than the second half which is further away from member 6.

In Figure 11g through Figure 11i, the influence of different external forces is examined as the initial length of member 6 is varied. For the five smaller force levels ($F = 1 \dots 20$ N), the trajectory curves are closed, and the shape of the enclosed area is elliptical for all three initial length levels (1 mm, 20 mm, and 45 mm). The overall movability of the structure increases symmetrically for all three cases. For high force levels $F = 35$ N and $F = 50$ N the overall stiffness changes in all three cases abruptly to a much smaller level, indicating more movability of the movable compressed member. On the left sides of the ellipses, a small part of the ellipses is shifted symmetrical to the inside ($F = 35$ N) and the outside ($F = 50$ N). With increasing initial length of the member 6, the points are placed corresponding to a more complex pattern, however also in these cases general elliptical forms can be observed. For a high initial length $L = 45$ mm, this effect already starts at an external force of $F = 20$ N but with only a small portion of the curve being shifted away.

In this section, the impact of the member's stiffness and initial length under consideration of different external force magnitudes on the overall mechanical behavior of the prestressed compliant structure was examined. As the results show, the investigations revealed that the initial stiffness of the tensioned members has a greater influence on the overall stiffness of the system compared to their initial length. For short member lengths, the structure's stiffness is nearly symmetrical in all directions (circle-like patterns). However, by increased member lengths, the stiffness will be more dependent on the force-direction (ellipsis-like patterns). The variation in member length directly affects the range of motion, with shorter members limiting and longer members enabling greater movability.

Regarding the member's stiffness, the nearly symmetrical behavior is observed only when the orthosis parameters are fully symmetrical. Adjusting the stiffness of selected members affects the direction-dependent stiffness of the system. Stiffer members restrict movement, while more softer members allow a wider range of motions in areas near to the members with modified stiffness. Both stiffer and softer tensioned members result in patterns that are shifted towards ellipses or crescent shapes. The orthosis can achieve a similar overall behavior by varying different tensioned members.

The examination of external forces acting on the orthosis demonstrates that for smaller forces, the overall structure behaves in an elliptical manner with symmetrical increases in form as the forces increase. It should be noted, that for large force magnitudes irregularities can arise, indicating possible multiple equilibrium solutions. In these cases, the form shifts towards crescent-shaped forms.

5. CONCLUSION

In this paper, a two-dimensional compliant tensegrity joint was investigated in context for possible further biomedical applications such as orthoses or exoskeletons. The structure consists of only two rigid compressed members, which are connected by five compliant tensioned members. The concept of the structure is based on the tensegrity principle. This principle enables the realization of dynamic orthoses without any conventional hinge joints. A further main advantage lies in the possibility of adaption to patient individual needs by proper design of the overall structure and by careful selection of member's properties. To analyze the mechanical behavior of the structure, the use of geometric nonlinear analysis was used. The overall static mechanical behavior with focus on the mechanical compliance of the considered structure was analyzed in dependence of structural parameters. The main objective was to determine the effect of the tensioned member's initial length and stiffness on the overall displacement of the movable member of the orthosis. It was demonstrated that the member's

parameters influence essentially the overall stiffness of the structure and their movability for given load magnitudes. The investigations laid the basis for the future development of dynamic orthoses based on this structure.

At this level of simulations, purely the basic structure of the orthosis was investigated. In summary, it can be stated that by proper design of member's parameters, the mechanical behavior of the orthosis can be defined according to individual patient needs.

Further work will focus on extended theoretical studies, including the underlying joint structure of the human hand. The overall static mechanical behavior of the orthosis will be calculated by using external forces corresponding to flexion/extension and radial/ulnar abduction in dependence of structural parameters. The long-term goal of future investigations is the physical realization of a passive orthosis demonstrator and their test for applicability in real settings.

REFERENCES

- [1] L. Schaeffer, D. Herrmann, and V. Boehm, "Preliminary Theoretical Considerations of a Hand Orthosis Based on a Prestressed, Compliant Structure," in 2023 International Symposium on Medical Robotics (ISMR), Atlanta, pp. 1–7, 2023. doi: 10.1109/ISMR57123.2023.10130230.
- [2] L. Schaeffer, D. Herrmann, and V. Böhm, "Voruntersuchung einer vorgespannten nachgiebigen Struktur für den Einsatz in dynamischen Handorthesen," Neunte IFToMM D-A-CH Konferenz 2023, Basel, 2023. doi: 10.17185/DUEPUBLICO/77392.
- [3] V. Böhm, "Mechanics of Tensegrity Structures and their Application in mobile Robotics," Habilitation thesis, Ilmenau University of Technology, Ilmenau, 2016.
- [4] T. Kaufhold, F. Schale, V. Böhm, and K. Zimmermann, "Indoor locomotion experiments of a spherical mobile robot based on a tensegrity structure with curved compressed members," in 2017 IEEE International Conference on Advanced Intelligent Mechatronics (AIM), Munich, pp. 523–528, 2017. doi: 10.1109/AIM.2017.8014070.
- [5] S. Sumi, V. Böhm, and K. Zimmermann, "A multistable tensegrity structure with a gripper application," Mechanism and Machine Theory, Ilmenau, Vol. 114, pp. 204–217, 2017. doi: 10.1016/j.mechmachtheory.2017.04.005.
- [6] P. Schorr, F. Schale, J. M. Otterbach, L. Zentner, K. Zimmermann, and V. Böhm, "Investigation of a Multistable Tensegrity Robot applied as Tilting Locomotion System," in 2020 IEEE International Conference on Robotics and Automation (ICRA), Paris, pp. 2932–2938, 2020. doi: 10.1109/ICRA40945.2020.9196706.
- [7] D. Zappetti, S. H. Jeong, J. Shintake, and D. Floreano, "Phase Changing Materials-Based Variable-Stiffness Tensegrity Structures," Soft Robotics, Vol. 7, No. 3, pp. 362–369, 2020. doi: 10.1089/soro.2019.0091.
- [8] V. Bohm, and K. Zimmermann, "Vibration-driven mobile robots based on single actuated tensegrity structures," in 2013 IEEE International Conference on Robotics and Automation (ICRA 2013), Karlsruhe, pp. 5475–5480, 2013. doi: 10.1109/ICRA.2013.6631362.
- [9] V. Böhm, S. Sumi, T. Kaufhold, and K. Zimmermann, "Compliant multistable tensegrity structures," Mechanism and Machine Theory, Ilmenau, Vol. 115, pp. 130–148, 2017. doi: 10.1016/j.mechmachtheory.2017.04.013.
- [10] D. Zappetti, S. Mintchev, J. Shintake, and D. Floreano, "Bio-inspired Tensegrity Soft Modular Robots," in 6th International Conference, Living Machines 2017, Stanford, pp. 497–508, 2017. doi: 10.1007/978-3-319-63537-8_42.
- [11] J. Rieffel, and J.-B. Mouret, "Adaptive and Resilient Soft Tensegrity Robots," Soft Robotics, Vol. 5, No. 3, pp. 318–329, 2018. doi: 10.1089/soro.2017.0066.
- [12] V. Böhm, P. Schorr, F. Schale, T. Kaufhold, L. Zentner, and K. Zimmermann, "Worm-Like Mobile Robot Based on a Tensegrity Structure," in 2021 IEEE 4th International

Conference on Soft Robotics (RoboSoft), New Haven, pp. 358–363, 2021. doi: 10.1109/RoboSoft51838.2021.9479193.

- [13] L.-Y. Zhang, Y. Li, Y.-P. Cao, and X.-Q. Feng, “Stiffness matrix based form-finding method of tensegrity structures,” *Engineering Structures*, Beijing, Vol. 58, pp. 36–48, 2014. doi: 10.1016/j.engstruct.2013.10.014.

CONTACTS

Leon Schaeffer M.Sc.
David Herrmann M.Sc.
Prof. Dr.-Ing. habil. V. Böhm

email: leon.schaeffer@oth-regensburg.de
email: david.herrmann@st.oth-regensburg.de
email: valter.boehm@oth-regensburg.de